Journal of
Synchrotron
Radiation

ISSN 1600-5775

Received 1 April 2014
Accepted 11 July 2014

Collateral circulation prevents masticatory muscle impairment in rat middle cerebral artery occlusion model

Falei Yuan,[a]‡ Xiaojie Lin,[a]‡ Yongjing Guan,[b] Zhihao Mu,[a,c] Kemin Chen,[b] Yongting Wang[a] and Guo-Yuan Yang[a,c]*

[a]Med-X Research Institute and School of Biomedical Engineering, Shanghai Jiao Tong University, Shanghai 200030, People's Republic of China, [b]Department of Radiology, Ruijin Hospital, School of Medicine, Shanghai Jiao Tong University, Shanghai 200025, People's Republic of China, and [c]Department of Neurology, Ruijin Hospital, School of Medicine, Shanghai Jiao Tong University, Shanghai 200025, People's Republic of China. *E-mail: gyyang0626@gmail.com

The rat suture middle cerebral artery occlusion (MCAO) is a frequently used animal model for investigating the mechanisms of ischemic brain injury. During suture MCAO, transection of the external carotid artery (ECA) potentially restrains blood flow and impairs masticatory muscle and other ECA-supported territories, consequently influencing post-operation animal survival. This study was aimed at investigating the effect of ECA transection on the hemodynamic alterations using a novel synchrotron radiation (SR) angiography technique and magnetic resonance imaging in live animals. Fifteen male adult Sprague-Dawley rats were used in this study. Animals underwent MCAO, in which the ECA was transected. SR angiography was performed before and after MCAO. Rats then underwent magnetic resonance imaging (MRI) to detect the tissue lesion both intra- and extra-cranially. Animals with SR angiography without other manipulations were used as control. High-resolution cerebrovascular morphology was analyzed using a novel technique of SR angiography. The masticatory muscle lesion was further examined by hematoxylin and eosin staining. MRI and histological results showed that there was no masticatory muscle lesion at 1, 7 and 28 days following MCAO with ECA transection. In normal condition, the ECA and its branch external maxillary artery were clearly detected. Following ECA transection, the external maxillary artery was still observed and the blood supply appeared from the anastomotic branch from the pterygopalatine artery. SR angiography further revealed the inter-relationship of hemisphere extra- and intra-cranial vasculature in the rat following MCAO. Transection of the ECA did not impair masticatory muscles in rat suture MCAO. Interrupted blood flow could be compensated by the collateral circulation from the pterygopalatine artery.

Keywords: angiography; collateral circulation; masticatory muscle; middle cerebral artery occlusion.

1. Introduction

Ischemic stroke is known as a leading cause of mortality and morbidity throughout the world. Currently, there are still no effective therapies available despite some promising advances in basic research. However, bench results often do not parallel with clinical outcomes. One of the reasons for this is the deviation of animal models. For instance, the rat suture model of middle cerebral artery occlusion (MCAO) has been widely accepted as a valid model, which mimics the human ischemic stroke (Koizumi *et al.*, 1986; Longa *et al.*, 1989); however, some disadvantages of the suture model have also been claimed such as premature reperfusion, subarachnoid hemorrhage, fluctuations of infarct volume and gradual loss of weight (Schmid-Elsaesser *et al.*, 1998; Boyko *et al.*, 2010; Guan *et al.*, 2012). These complications are likely to affect the results of experimental animal ischemic stroke for further therapeutic interventions.

The common carotid artery (CCA) branches into the external carotid artery (ECA) and the internal carotid artery (ICA). The ICA then gives off the pterygopalatine artery

‡ These authors contributed equally to this work.

(PPA) and its intra-cranial branches. The ECA is the major blood supplying artery of masticatory muscles in rats. Generally, ECA transection is necessary for the suture model to insert the suture from the ECA stump, and reperfusion can also be achieved by withdrawing the suture to the stump. The impact of ECA transection on masticatory muscles is a topic of continuous debate. In 2003, Dittmar *et al.* reported the impairment of masticatory and temporal muscle after suture-induced MCAO in Wistar rats (Dittmar *et al.*, 2003). The same complications were also observed in Sprague-Dawley rats (Palmer *et al.*, 2001). The loss of body weight was attributed to the impairment of the masticatory muscle by ECA transection. Thus, a lot of effort has been made to optimize the suture model in order to prevent ischemic injury of the ECA territory from ischemia (Dittmar *et al.*, 2005*a*; Boyko *et al.*, 2010). Nevertheless, Gerriets and associates re-evaluated the ischemia of temporal muscle by using three different rat stroke models, concluding that there were no muscle hyper-intensities in both Wistar rats and Sprague-Dawley rats after MCAO (Dittmar *et al.*, 2005*b*).

Weight loss after stroke was continually reported in a large number of ischemic studies; however, this important phenomenon has attracted little attention and has never been formally studied (Dirnagl, 2010). The impairment of masticatory muscles is frequently described as the most important factor for low survival rates and gradual weight loss, yet the correlation between intra- and extra-cranial blood supply after MCAO remains obscure. Synchrotron radiation (SR) imaging in *ex vivo* tissue and *in vivo* small animals has been developed over the past 15 years (Shirai *et al.*, 2013; Popescu *et al.*, 2011). The high resolution of SR angiography enables researchers to dynamically investigate the intra- and extra-cranial microcirculation in rodents (Shirai *et al.*, 2013). The purpose of the present study was to explore the effect of the blood supply alteration and the collateral opening on the injury of masticatory muscle in a rat intraluminal suture MCAO model.

2. Materials and methods

2.1. Experimental design

Animal surgical procedures and experimental protocols were reviewed and approved by the Institutional Animal Care and Use Committee (IACUC) and the Bioethics Committee of the School of Biomedical Engineering, Shanghai Jiao Tong University, Shanghai, China. Fifteen adult male Sprague-Dawley rats (Sppir-BK Inc., Shanghai, China) weighing 250–280 g were used in this study. Animals underwent magnetic resonance imaging (MRI) before and 1, 7 and 28 days after MCAO to detect the tissue lesion intra- and extra-cranially. SR angiography was performed before and after ECA transection. Animals characterized with SR angiography without MCAO were used as control.

2.2. Surgical procedure

The surgical procedure for MCAO has been described previously (Yang & Betz, 1994). In short, rats were anesthetized with ketamine (100 mg kg^{-1}) and xylazine (10 mg kg^{-1}) intraperitoneally. Animals were then placed supinely on a heating pad maintaining body temperature at 310 ± 0.5 K. The left CCA, ECA and ICA were isolated under an operating microscope (Leica; Wetzlar, Germany). After ECA transection, a silicone-coated 4-0 suture (Dermalon, 1756-31, Covidien, OH, USA) was inserted into the ECA stump and advanced from the ICA to the ostium of the MCA until a slight resistance was felt. Body weight was measured before and 1, 3, 7, 14 and 28 days after MCAO.

2.3. Magnetic resonance imaging

After MCAO, rats were re-anesthetized with ketamine/xylazine intraperitoneally. MRI examination of brain and neck were performed before and after the operation using a 3 T MR apparatus (GESigna3T; GE Healthcare, CT, USA) using an animal head coil with T2-weighted fast spin-echo sequence (time of repetition = 5840 ms, time of echo = 106 ms, field of view = 60 mm × 60 mm, matrix = 256 × 256, slice thickness = 1.5 mm, four collections). T2-weighted images were obtained before and 1, 7 and 28 days after MCAO. Brightness and contrast were adjusted for optimal display of the tissue.

2.4. SR angiography

SR angiography was conducted at beamline BL13W at Shanghai Synchrotron Radiation Facility (SSRF). Imaging parameters and procedures have been described previously (Yuan *et al.*, 2012). An average beam current of 145 mA and X-ray energy of 33.2 keV was used. A custom-made T-shaped catheter, formed by connecting a PE-10 tube with a PE-50 tube, was invasively embedded into the CCA prior to imaging.

Then, the rat was placed vertical to the beam on its left side, and 150 µl of contrast agent (Ipamiro, Shanghai, China) with a concentration of 175 mgI ml^{-1} (350 mgI ml^{-1}, diluted to 50% volume ratio with saline) was injected into the CCA through the T-tube at an injecting rate of 133.3 µl s^{-1} using a microsyringe pump (Longer; Baoding, China). A PCO X-ray CCD camera (pixel size 9 µm × 9 µm; PCO-TECH Inc., Germany) was used to obtain high-resolution real-time angiographic images. The CCD camera was placed 65 cm away from the sample stage.

2.5. Hematoxylin and eosin staining

Animals were anesthetized after SR angiography and perfused with saline followed by 4% paraformaldehyde transcardially. The masticatory muscle was fixed in 4% paraformaldehyde for 24 h and dehydrated using a graded alcohol system and then embedded in paraffin. Paraffin sections of thickness 6 µm were prepared for hematoxylin and eosin staining according to our previous study (Lin *et al.*, 2013).

2.6. Image analysis

MR images were read and described by two experienced radiologists using the double-blind method. The MRI intensities in the left and right masticatory muscle were counted

using *Image-Pro Plus* 6.0 software (Media Cybernetics, Rockville, MD, USA). The normalized MRI intensity of masticatory muscle was calculated as dividing the left masticatory muscle by the right masticatory muscle. For SR angiography, ten consecutive images taken before contrast enhancement were subtracted from raw images taken after injection to eliminate the background structure. Images were post-processed using *MatLab2010a* (The MathWorks Ltd, Natick, MA, USA) to perform a temporal subtraction. To acquire a clear general view of the rat cerebrovascular system, the Adobe *Photoshop* program (Adobe, San Jose, CA) was used to montage multi-section radiographs.

2.7. Statistical analysis

Data for the body weight were presented as mean ± standard deviation (SD). The normalized MRI intensities among different groups were compared using a two-way ANOVA followed by Student's t-test. A probability value of less than 5% was considered statistically significant.

3. Results

3.1. Body weight was affected by MCAO surgery

The body weight of all animals significantly decreased from day 1 to day 3 and gradually recovered from day 7 to day 28 after MCAO (Fig. 1). This result indicates that body weight is related to MCAO and ECA transection. Absence of apparent masticatory muscle damage excludes the impairment to chewing ability as an underlying cause for the weight loss. Other factors from MCAO-induced ischemia should be considered.

3.2. MCAO surgery did not impair blood flow to the masticatory muscle territory

The results of T2-weighted MRI showed lower signal density in the left masticatory muscle in rats before and 1, 7 and 28 days after MCAO with ECA transection. No hyperintense signal was found in the left masticatory muscle territory in the experimental rats. There was no statistically significance of MRI intensity between left and right masticatory muscle, and also no significance of normalized MRI intensity among rats before and 1, 7 and 28 days after MCAO with ECA transection (Fig. 2).

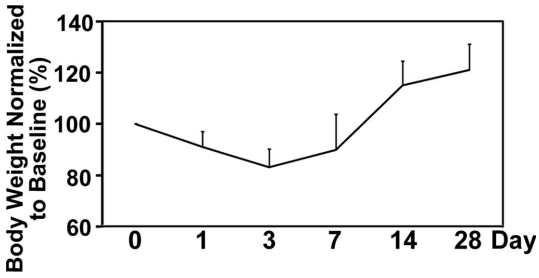

Figure 1
Body weight alterations after MCAO with ECA transection. Normalized body weight was calculated by dividing the weight on each day by the baseline. Data are presented as mean ± SD, $n = 6$ per time point.

Hematoxylin and eosin staining showed regular alignment of smooth muscle cells in the left masticatory muscle of rats (Fig. 2). These results indicated that the masticatory muscle was not affected after ECA transection during the MCAO procedure, and the body weight loss was not due to the damage of masticatory muscle after suture-induced MCAO.

3.3. Anastomoses from the PPA to external maxillary artery maintain blood flow of the ECA after ECA transection

SR angiography showed that the PPA and ICA were clearly revealed in rats with or without ECA transection. Interestingly, the external maxillary artery (EMA), a major branch of the ECA providing blood flow to the masticatory muscle, was revealed with or without ECA transection (Fig. 3). According to the dynamic images obtained by SR angiography, the blood flow in the EMA was supplied from the anastomotic branch to palatine (ABTP), indicating that collateral circulation was established (Figs. 3 and 4).

These results suggested that the ECA territory would not be affected after ECA transection during MCAO surgery. Therefore, these anastomoses could maintain the integrity of the masticatory muscle.

4. Discussion

In the current study we investigated the correlation between intra- and extra-cranial blood supply in a rat suture MCAO model. We demonstrated that the transection of the ECA did not lead to injury of the masticatory muscles after MCAO. We also provided direct *in vivo* evidence of anastomoses between the PPA and the EMA (a branch of the ECA), which is consistent with the previous meticulous work performed by Greene nearly 80 years ago (Greene, 1936). The existence of these collaterals accounts for the viability of the transection of the ECA in this model.

SR angiography has been developed as an effective tool for angiography in small animals. Studies on the circulation alteration and blood vessel dilation of brain after ischemia have been continuously reported in both rats and mice (Kidoguchi *et al.*, 2006). Here we used a T-shaped catheter that was embedded in the CCA for injecting the contrast agent. The T-shaped catheter enabled us to detect the vasculature of the entire brain including the extra-cranial part without interrupting the blood flow to the ECA territory. Regular cannulation was usually performed by inserting a PE-10 catheter into the ECA stump, and interruption of the ECA blood flow was inevitable with this technique. Intraluminal suture insertion often leads to endothelium denudation, followed by platelet aggregation and smooth muscle cells proliferation. Surgery-related thrombosis and post-operative stenosis presumably influence the reproducibility of suture MCAO models (Lin *et al.*, 2013). The emboli moved around randomly as shown by SR angiography.

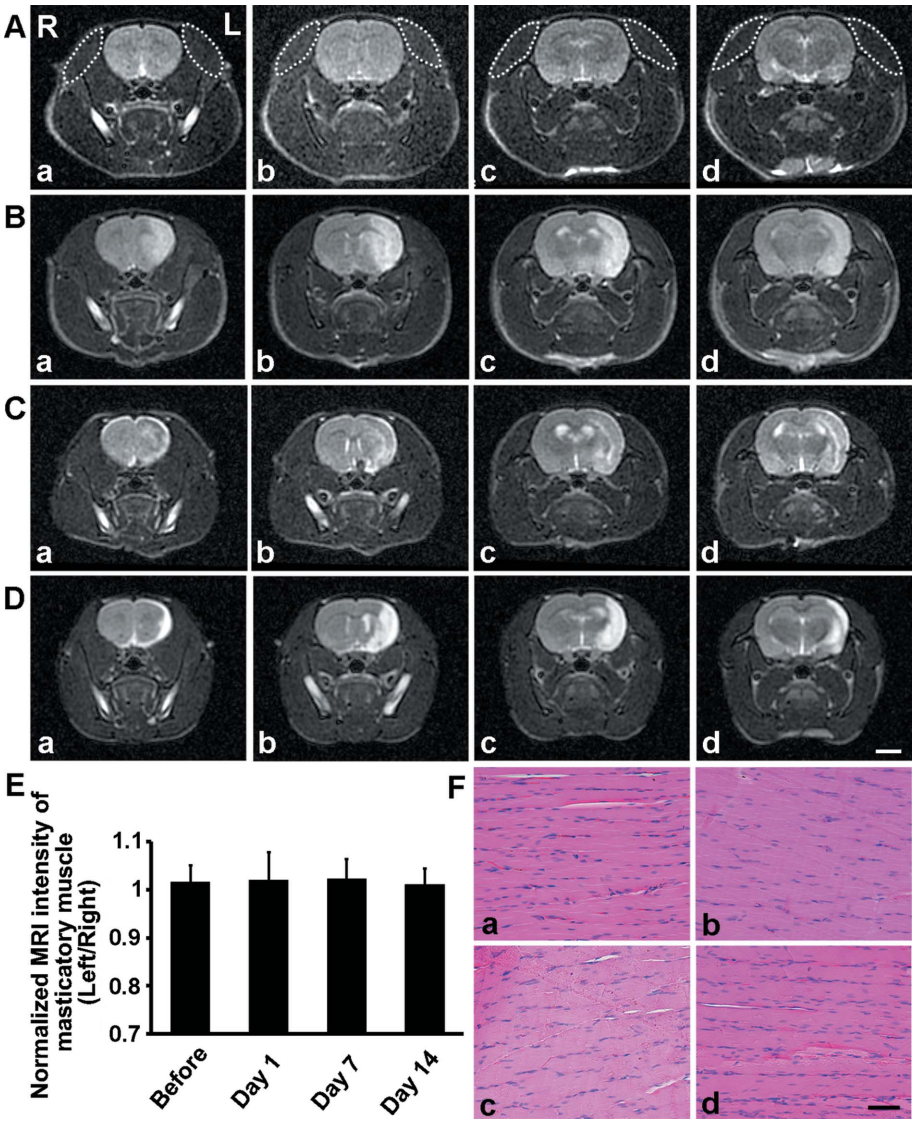

Figure 2
T2-weighted MRI showing the masticatory muscle and brain tissue morphology before (A) and 1 (B), 7 (C) and 28 (D) days post MCAO, and the normalized MRI intensity of the masticatory muscle (E). Coronal sections from anterior to posterior show that there was no extra-cranial injury in A–D. Dotted circles show the left or the right masticatory muscle. High-intensity signal indicates tissue lesion after ischemia. (F) Hematoxylin and eosin staining of the masticatory muscle in rats before (*a*) and 1 (*b*), 7 (*c*) and 28 (*d*) days after MCAO. R: right hemisphere; L: left hemisphere. Scale bar: 4 mm (A–D); 50 µm (F).

Stroke is known as a wasting disease and cachexia after stroke has been frequently documented clinically and experimentally (Scherbakov *et al.*, 2011; Meisel *et al.*, 2004). Weight loss can reach up to 20% in rodent stroke models; the cause of gradual weight loss has yet to be revealed (Dirnagl, 2010). Suture models of MCAO are always accompanied by occlusion of the hypothalamic artery, which might give rise to increased body temperature and impaired feeding. According to our previous experience, the high mortality of mouse MCAO model is associated with the variation of the posterior communicating artery (PcomA) (Yuan *et al.*, 2012). Weight loss, therefore, could be affected by the development of the PcomA because the PcomA functioned as a major tributary to the thalamus, hypothalamus and hippocampus when the posterior cerebral artery was completely or partially occluded by the suture (Coyle, 1975). These critical structures are responsible for body temperature adjustment and feeding behaviors. When infarct or under hypo-perfusion, they could possibly result in the disparities in post-operative recovery in rat suture MCAO.

Further studies should focus on other factors affecting animal survival in rat suture models such as the correlation between the diameters of the ipsilateral PcomA and the body weight loss.

The authors thank Dr Tiqiao Xiao of BL13W station at SSRF. This study was supported by the National Basic Research Program (973 Program) 2010CB834306 (GYY, YW), the National Natural Science Foundation of

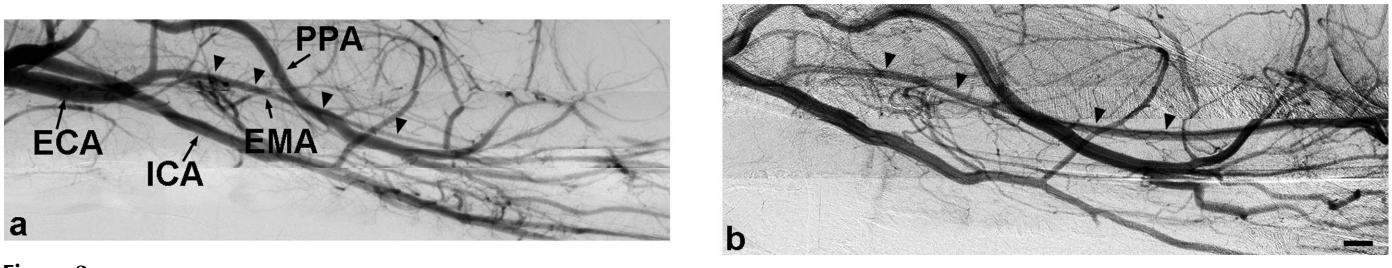

Figure 3
SR angiography images showing the intra- and extra-cranial vasculature morphology without (*a*) and with (*b*) transecting the external carotid artery (ECA). A T-shaped catheter was introduced to perform SR imaging of the entire cranial vasculature including territories supplied by the ECA. The ECA and its downstream branch EMA were clearly detected when the ECA was still intact (*a*). After ligating the ECA, a retroverse blood flow from PPA perfused the ECA territory, indicating the possibility of collaterals from the PPA sparing the tissue supplied by the ECA from extra-cranial ischemia (*b*). ICA: internal carotid artery; EMA: external maxillary artery; PPA: pterygopalatine artery. Scale bar: 1 mm.

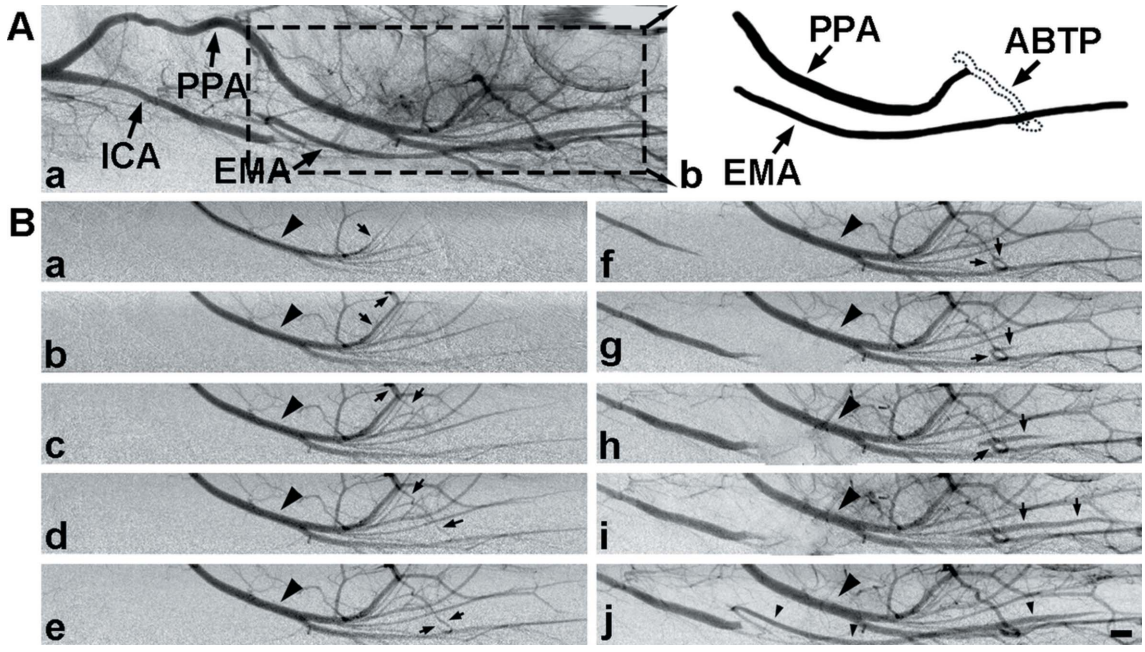

Figure 4
Dynamic images of SR angiography showing the collateral circulation between the external maxillary artery (EMA) and the pterygopalatine artery (PPA) after external carotid artery transection. (A) SR angiography imaging (*a*) in rat after ECA transection and middle cerebral artery occlusion and (*b*) diagram of the anastomoses between the PPA and the EMA. (B) The dynamic figures with contrast enhancement (*a–j*) showing the time course of EMA appearance after ECA transection performed by SR angiography. The images show that the contrast agent flowed from the PPA (large arrowheads) to the EMA (small arrowheads) through the ABTP (arrows). ICA: internal carotid artery. Scale bar: 1 mm.

China U1232205 (GYY) and Shanghai Jiao Tong University Foundation for technological innovation of major projects 12X190030021 (GYY), the Science and Technology Commission of Shanghai Municipality programs 13140903500 (GYY).

References

Boyko, M., Zlotnik, A., Gruenbaum, B. F., Gruenbaum, S. E., Ohayon, S., Goldsmith, T., Kotz, R., Leibowitz, A., Sheiner, E. & Shapira, Y. (2010). *J. Neurosci. Methods*, **193**, 246–253.
Coyle, P. (1975). *Exp. Neurol.* **49**, 671–690.
Dirnagl, U. (2010). *Rodent Models of Stroke.* New York: Springer.
Dittmar, M., Spruss, T., Schuierer, G. & Horn, M. (2003). *Stroke*, **34**, 2252–2257.
Dittmar, M. S., Fehm, N. P., Vatankhah, B., Bogdahn, U., Schlachetzki, F., Gerriets, T., Stolz, E., Kaps, M., Walberer, M. & Mueller, C. (2005*b*). *Stroke*, **36**, 530.
Dittmar, M. S., Vatankhah, B., Fehm, N. P., Retzl, G., Schuierer, G., Bogdahn, U., Schlachetzki, F. & Horn, M. (2005*a*). *Exp. Neurol.* **195**, 372–378.
Greene, E. C. (1936). *Am. J. Med. Sci.* **191**, 858.
Guan, Y., Wang, Y., Yuan, F., Lu, H., Ren, Y., Xiao, T., Chen, K., Greenberg, D. A., Jin, K. & Yang, G. Y. (2012). *Stroke*, **43**, 888–891.
Kidoguchi, K., Tamaki, M., Mizobe, T., Koyama, J., Kondoh, T., Kohmura, E., Sakurai, T., Yokono, K. & Umetani, K. (2006). *Stroke*, **37**, 1856–1861.
Koizumi, J., Yoshida, Y., Nakazawa, T. & Ooneda, G. (1986). *Jpn. J. Stroke*, **8**, 1–8.
Lin, X., Miao, P., Wang, J., Yuan, F., Guan, Y., Tang, Y., He, X., Wang, Y. & Yang, G.-Y. (2013). *PLoS One*, **8**, e75561.
Longa, E. Z., Weinstein, P. R., Carlson, S. & Cummins, R. (1989). *Stroke*, **20**, 84–91.
Meisel, C., Prass, K., Braun, J., Victorov, I., Wolf, T., Megow, D., Halle, E., Volk, H.-D., Dirnagl, U. & Meisel, A. (2004). *Stroke*, **35**, 2–6.
Palmer, G. C., Peeling, J., Corbett, D., Bigio, M. R. & Hudzik, T. J. (2001). *Ann. New York Acad. Sci.* **939**, 283–296.
Popescu, G., Florin, B. & Nichol, H. (2011). *CNS Neurosci. Ther.* **17**, 256–268.
Scherbakov, N., Dirnagl, U. & Doehner, W. (2011). *Stroke*, **42**, 3646–3650.
Schmid-Elsaesser, R., Zausinger, S., Hungerhuber, E., Baethmann, A. & Reulen, H. J. (1998). *Stroke*, **29**, 2162–2170.
Shirai, M., Schwenke, D. O., Tsuchimochi, H., Umetani, K., Yagi, N. & Pearson, J. T. (2013). *Circ. Res.* **112**, 209–221.
Yang, G.-Y. & Betz, A. L. (1994). *Stroke*, **25**, 1658–1664.
Yuan, F., Tang, Y., Lin, X., Xi, Y., Guan, Y., Xiao, T., Chen, J., Zhang, Z., Yang, G. Y. & Wang, Y. (2012). *J. Neurotrauma*, **29**, 1499–1505.